Controlling the Incorporation and Release of C_{60} in Nanometer-Scale Hollow Spaces inside Single-Wall Carbon Nanohorns

Ryota Yuge,*,† Masako Yudasaka,*,†,‡ Jin Miyawaki,‡ Yoshimi Kubo,† Toshinari Ichihashi,† Hideto Imai,† Eiichi Nakamura,§,|| Hiroyuki Isobe,§,⊥ Hideki Yorimitsu,§ and Sumio Iijima#

Fundamental and Environmental Research Laboratories, NEC Corporation, 34 Miyukigaoka, Tsukuba 305-8501, Japan, SORST, Japan Science and Technology Agency, c/o NEC Corporation, 34 Miyukigaoka, Tsukuba 305-8501, Japan, Department of Chemistry, University of Tokyo, Hongo, Bunkyo-ku, Tokyo 113-0033, Japan, ERATO, Japan Science and Technology Agency, PRESTO, Japan Science and Technology Agency, Meijo University, 1-501 Shiogamaguchi, Nagoya 468-8502, Japan

Received: May 27, 2005; In Final Form: August 2, 2005

We succeeded in large-scale preparation of single-wall carbon nanohorns (SWNH) encapsulating C_{60} molecules in a liquid phase at room temperature using a "nano-precipitation" method, that is, complete evaporation of the toluene from a C_{60}−SWNH−toluene mixture. The C_{60} molecules were found to occupy 6−36% of the hollow space inside the SWNH, depending on the initial quantity of C_{60}. We showed that the C_{60} in C_{60}@SWNHox was quickly released in toluene, and the release rate decreased by adding ethanol to toluene. Numerical analysis of the release profiles indicated that there were fast and slow release processes. We consider that the incorporation quantity and the release rate of C_{60} were controllable in/from SWNHs because SWNHs have large diameters, 2−5 nm.

Introduction

The functions of single-wall carbon nanotubes (SWNTs) are likely to be expanded by the incorporation of functional materials. Various materials have been incorporated in SWNTs,[1−8] though as yet little functionality has actually been exhibited. This situation is probably due partly to the lack of methods for incorporating materials in a large quantity of SWNTs and partly to the immaturity of the technologies required to control the amount of filling materials and the rate of their releases.

To incorporate materials into a large quantity of SWNTs, liquid-phase incorporation is useful, though not much has been studied.[9−11] We previously reported an incorporation method carried out in liquid phase at room temperature, named as "nano-extraction",[9] in which a material dissolved in a poor solvent is extracted inside the SWNTs. To make this method effective, the affinity among the material, solvent, and SWNTs needs to be balanced, which inhibits the wide applicability of "nano-extraction". To overcome this problem, we propose, in this report, to apply a "nano-precipitation" method, that is, dispersion of nanotubes in a solution of guest materials, followed by complete evaporation of the solvent. Since this method does not require any strict conditions on the affinity balances, it would be applicable to the encapsulation of various materials inside SWNTs. It is noteworthy that this method, like "nano-extraction", can be carried out at room temperature in the liquid phase and is therefore suitable for encapsulating even thermally unstable molecules. To demonstrate that "nano-precipitation" is useful, we applied this method to the incorporation of C_{60} inside single-wall carbon nanohorns (SWNHs). We found that it was possible to incorporate C_{60} and, moreover, that the filling quantity and release rates of C_{60} were controllable, results of which are shown in this report. The SWNH is a type of SWNT, but it has larger diameters of 2−5 nm.[12] SWNHs gather and form spherical aggregates with diameters of about 80−100 nm.[12] They are closed tubes in the as-grown states, but holes are easily opened by combustion with oxygen.[13−15] The holes are known to allow fullerenes and other molecules to enter inside the SWNHs.[13−19]

Experimental Section

SWNH aggregates were prepared using a CO_2 laser ablation method.[12] The purity was 85−90%, and the impurities were micrometer-sized graphite-based particles. The SWNH aggregates were heat-treated at 550 °C for 10 min in oxygen flow (760 Torr, 200 cm^3 min^{-1}). With this oxygen-gas treatment, the tip and defect sites of the SWNHs were locally combusted and holes were pierced through the walls. In this study, oxidation-treated SWNHs were labeled as SWNHox.

The "nano-precipitation" process is shown in Figure 1a. The material incorporated was C_{60}, and its quantity against SWNHox varied from 1 to 60% (Table 1). The percent in this report means the mass percent (C_{60}/(C_{60} + SWNHox)), unless otherwise stated. We put the SWNHox into a C_{60}−toluene solution, and ultrasonicated the SWNHox−C_{60}−toluene mixtures for 1 min to disperse the SWNHox homogeneously. The toluene was then evaporated from the C_{60}−SWNHox−toluene mixture at room temperature in a nitrogen atmosphere (760 Torr). The specimen thus obtained is called C_{60}@SWNHox in this report.

The quantity of incorporated C_{60} was estimated using thermogravimetric (TG) measurements carried out in an oxygen atmosphere (760 Torr, 100 cm^3 min^{-1}) from room temperature to 1000 °C with a ramp rate of 5 °C min^{-1}. A constant amount

* Corresponding authors. E-mail: yudasaka@frl.cl.nec.co.jp (Yudasaka), ryuge@frl.cl.nec.co.jp (Yuge).
† Fundamental and Environmental Research Laboratories, NEC Corporation.
‡ SORST, Japan Science and Technology Agency, c/o NEC Corporation.
§ Department of Chemistry, University of Tokyo.
|| ERATO, Japan Science and Technology Agency.
⊥ PRESTO, Japan Science and Technology Agency.
Meijo University.

10.1021/jp052814d CCC: $30.25
Published on Web 09/01/2005

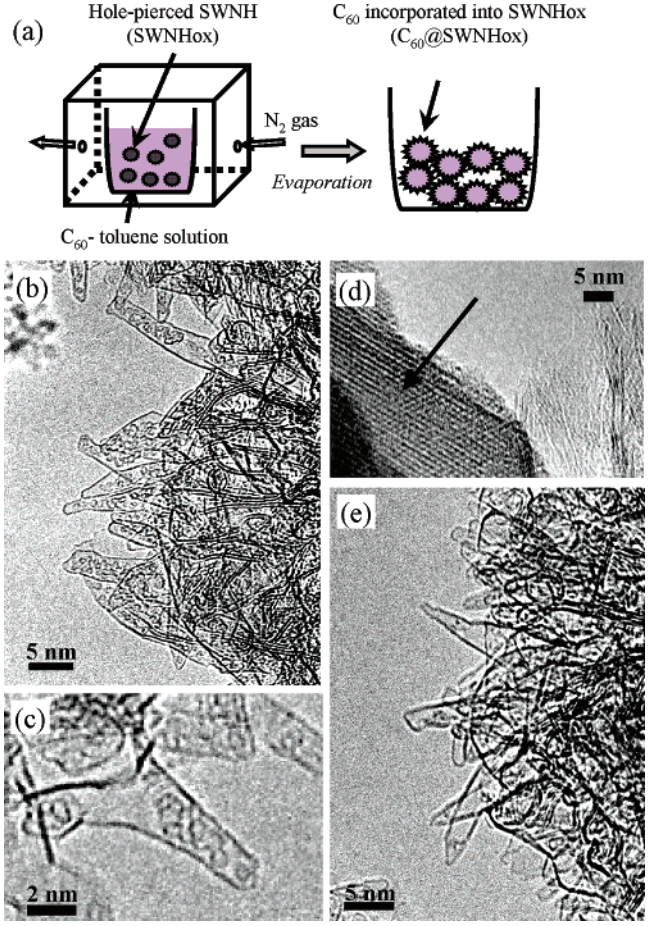

Figure 1. Schematic illustration of nano-precipitation method (a). TEM images of C_{60}@SWNHox prepared by nano-precipitation (b and c), and C_{60} crystal (indicated by arrow) deposited on as-grown SWNHs (d). TEM image of residue obtained by stopping TG measurement of 15%-C_{60}@SWNHox at 500 °C, indicating most of the C_{60} was eliminated by combustion with O_2 (e).

TABLE 1: Filling Factors Controlled by the Initial C_{60} Quantities. Quantities of C_{60} Incorporated Inside SWNHox Were Controlled by Adjusting the Initial Quantities of C_{60} against SWNHox. The Solvent Was Toluene[a]

starting quantity of C_{60}	%[b]	1	3	10	15	40	60
in the initial mixture of C_{60},	g/g[c]	0.01	0.03	0.11	0.18	0.67	1.50
SWNHox, and toluene	vol/vol[d]	0.02	0.05	0.17	0.28	1.06	1.65
ratio of incorporated C_{60} and	g/g[c]	0	0.03	0.09	0.11	0.22	*e*
SWNHox in the end	vol/vol[d]	0	0.05	0.15	0.19	0.36	*e*
products of C_{60}@SWNHox							

[a] The quantities of incorporated C_{60} were estimated from TG curves (Figure 2a). In calculating C_{60} quantities in units of vol/vol, the density of the C_{60} crystal (1.68 g cm^{-3}) and the pore volume of the inside space of the SWNHox (0.36 mL g^{-1})[13] were applied. [b] %: $C_{60}/(C_{60}$ + SWNHox) × 100. [c] g/g: weight ratio of C_{60} and SWNHox. [d] vol/vol: volume ratio of C_{60} and SWNHox. [e] Since part of the C_{60} was outside the SWNHox, the quantity of incorporated C_{60} could not be estimated from the TG data.

(ca. 1.4 mg) of samples was used for the TG measurements. To confirm whether C_{60} was incorporated inside the SWNHs, the C_{60}@SWNHox was observed with a transmission electron microscope (TEM) (Topcon, EM-002B) operated at a 120 kV accelerating voltage. X-ray diffraction (XRD) was measured using Cu Kα radiation with the 40-kV accelerating voltage and 40-mA beam current. Raman spectra (30 min for one spectrum measurement) were measured with a Jasco NRS-2000 Laser Raman spectrophotometer. The excitation wavelength was 488.0 nm, and its intensity at the sample was about 100 W cm^{-2}. The UV/vis absorption spectra were measured to estimate the quantity of C_{60} released from the C_{60}@SWNHox into the solvents (toluene, ethanol, and a toluene−ethanol mixture). In this observation, C_{60}@SWNHox was dispersed in 300 cm^3 of these solvents at a concentration of 7 mg L^{-1}. The solution was held in closed containers for periods ranging from 2 to 100 h, during which 5 cm^3 of the supernatant was sucked out and the UV/vis spectrum was measured. The measured amount (5 cm^3) was then returned to the source solution.

Results and Discussion

Controlling the Quantity of C_{60} Incorporated inside SWNHox. As a result of "nano-precipitation", the C_{60} molecules were incorporated inside the SWNHox, which was confirmed by TEM observation (Figure 1b,c). C_{60} was never incorporated inside as-grown SWNHs because these did not have holes. When we applied "nano-precipitation" of C_{60} to the as-grown SWNHs, the C_{60} crystallized by itself on the outside walls of the as-grown SWNHs. A TEM image of the C_{60} crystal is indicated by an arrow in Figure 1d where the crystal lattice is clearly visible.

We estimated the quantity of incorporated C_{60} through TG measurements of the C_{60}@SWNHox. The measured TG and its derivative (DTG) curves are shown in Figure 2a. The DTG curves indicate that C_{60}, SWNHox, and the graphitic byproduct combusted at different temperatures. The SWNHox and graphite-like particles (byproduct) combusted at about 620 and 730 °C, respectively.[20] The C_{60} molecules in C_{60}@SWNHox burned in the temperature range from 320 to 530 °C, which was confirmed by the fact that the SWNHox obtained by stopping the TG measurement at 500 °C was empty (Figure 1e). This suggests that the disappearance of C_{60} during TG measurement up to 500 °C was due to its combustion inside the SWNHox with the oxygen that had permeated into the inside of SWNHox. We also found that sublimation of C_{60} could not account for this disappearance because no weight decrease was observed in the TG measurement in helium up to 500 °C, and TEM observation of the 500 °C residue (Supporting Information) showed that there was often C_{60} inside the SWNHox, while some of which were structurally deformed.

The quantities of C_{60} per unit quantity of the SWNHox were estimated from the decreases in weight from 320 to 530 °C (Figure 2a) and are summarized in Table 1. In preparing C_{60}@SWNHox, some amount of C_{60} adsorbed or deposited on the inner wall of the sample container during the evaporation of the solvent. As a result, the quantity ratio of C_{60} and SWNHox became higher in the starting material than in the resulting material (Table 1). As the starting quantity of C_{60} compared to that of SWNHox increased, the quantity of incorporated C_{60} increased, and about 36% of the interior space was filled with C_{60} when the initial C_{60} concentration was 40% (weight). These results indicate that the quantity of C_{60} incorporated inside the SWNHox can be controlled simply by varying the starting quantity of C_{60}.

Since the combustion-temperature range of the C_{60} molecules of the C_{60}@SWNHox (Figure 2a) was overlaid with that of the C_{60} crystallites deposited outside the as-grown SWNHs (Figure 2b), we examined whether C_{60} existed inside or outside the SWNHox through XRD and Raman spectrum measurements of the C_{60}@SWNHox.

The XRD profiles of C_{60}-deposited as-grown SWNHs (Figure 3e) exhibited diffraction peaks corresponding to C_{60} crystals (111), (220), and (311) (Figure 3f). The relative intensities of these peaks were different. Especially, in the case of the XRD

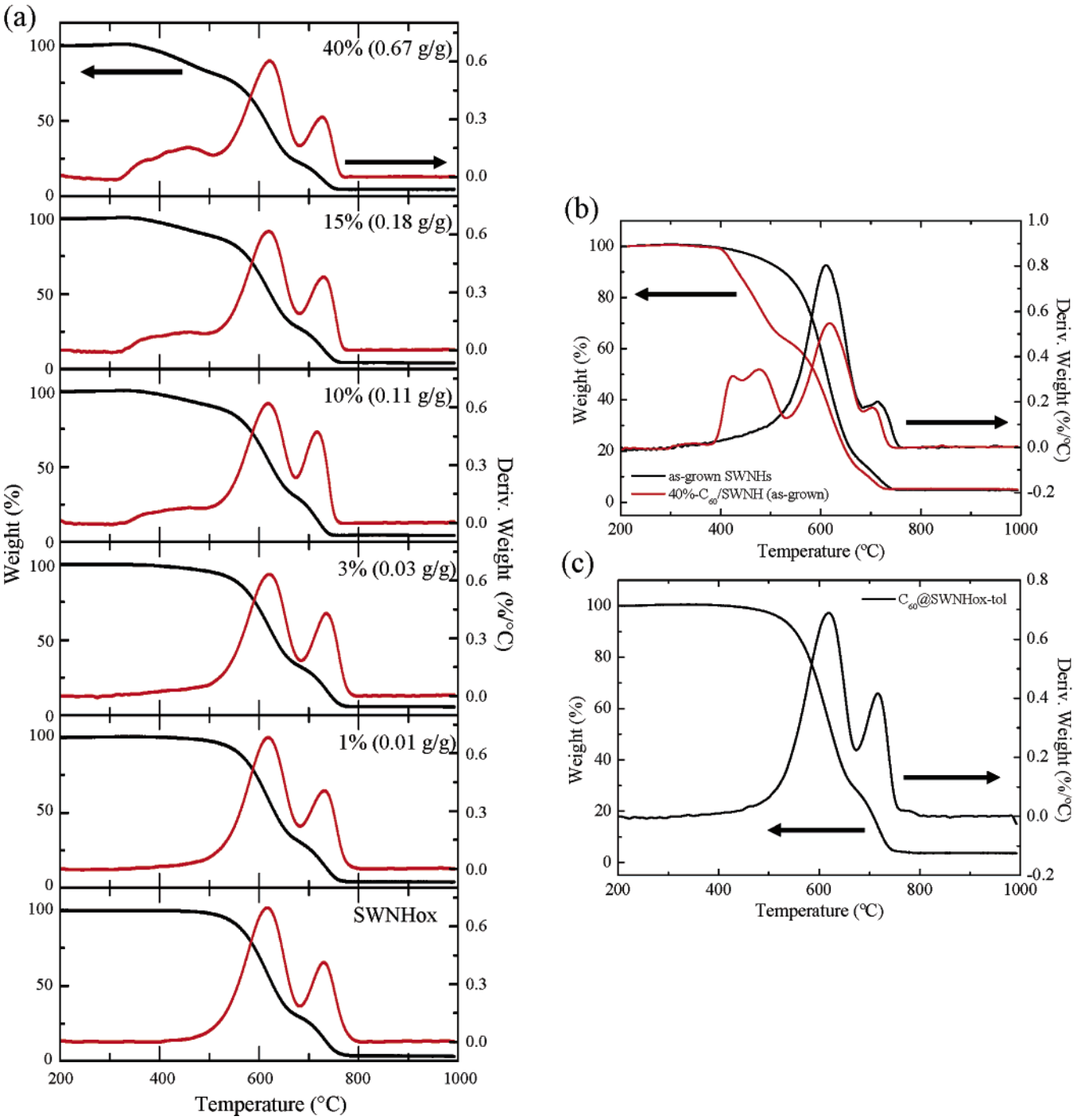

Figure 2. TG and DTG profiles of C_{60}@SWNHox, when the initial quantities of C_{60} were about 0, 1, 3, 10, 15, and 40% (a). TG and DTG profiles of as-grown SWNHs (black), and 40%-C_{60}/SWNHs (as-grown) (red) (b). TG and DTG profiles of C_{60}@SWNHox immersed in toluene for 30 min (C_{60}@SWNHox-tol) (c). (The residual weights at 1000 °C were due to the background, which differed in each measurement. We did not find anything remaining in the pan after the TG measurement, meaning C_{60} and SWNHox were completely burned.)

profiles of the C_{60}-deposited as-grown SWNHs, the (220) peak was very strong, while the others were very weak (Figure 3e), indicating that the (220) face of the C_{60} crystals was the preferential orientation on the surfaces of SWNHox, though we do not discuss this in detail in this report. When the starting quantity of C_{60} was as high as 60%, XRD peaks corresponding to the neat-C_{60} crystals were also seen (Figure 3d). However, no peaks corresponding to the neat-C_{60} crystals were observed when the starting C_{60} quantity decreased to 40% or less (Figure 3b,c). These results indicate that the excess C_{60} molecules crystallized outside the SWNHox and exhibited peaks corresponding to the neat-C_{60} crystal, while when the C_{60} molecules were encapsulated inside the SWNHox, no XRD peaks ascribed to the C_{60} crystals appeared due to the small size of the crystals or poor crystallites. A peak and shoulder near 26° corresponded to periodic structures with a spacing of 3.44 and 3.36 nm, which is close to those of graphite with a turbostratic structure.[21] We ascribed these peaks to the diffractions from the graphitic particles (byproducts of SWNH).[20] The shoulder became more pronounced for SWNHox, perhaps because the thermal annealing effect to the graphitic particles worked during the heat treatment in O_2.

The Raman spectra of the C_{60}@SWNHox exhibited a peak at 1466 cm^{-1} corresponding to the A_{2g} "pentagonal pinch"

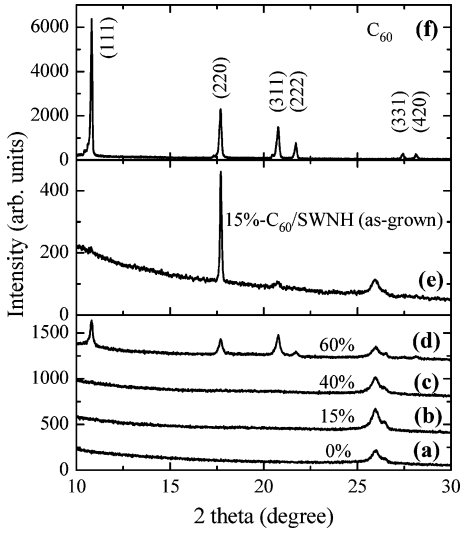

Figure 3. X-ray diffraction patterns of SWNHox (a), 15%-C_{60}@SWNHox (b), 40%-C_{60}@SWNHox (c), 60%-C_{60}@SWNHox (d), 15%-C_{60}/as-grown SWNHs (e), and C_{60} powder (f). The peak at 25.8° and the shoulder at 26.3° are of graphite-like particles (byproducts of SWNHs).[20]

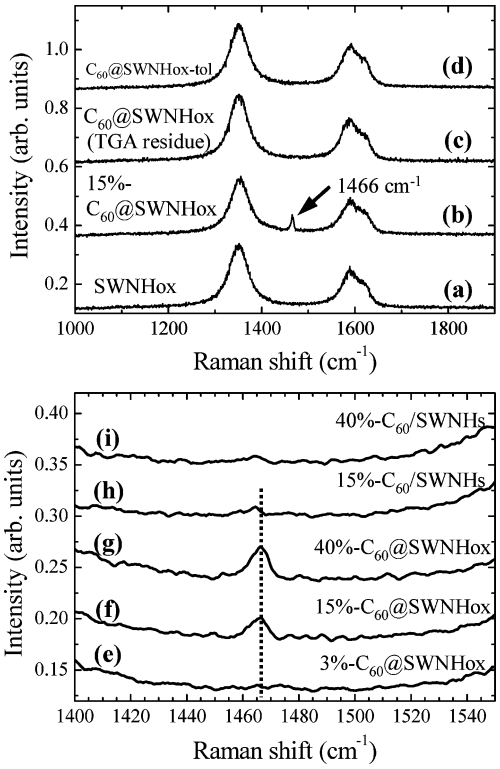

Figure 4. Raman spectra of SWNHox (a), 15%-C_{60}@SWNHox (b), residue obtained by stopping TG measurement of 15%-C_{60}@SWNHox at 500 °C (c), and 15%-C_{60}@SWNHox after immersing in toluene for 30 min (d). Raman peaks at 1466 cm^{-1} corresponding to the A_{2g} vibration mode of C_{60} were observed in the spectra of 15%- and 40%-C_{60}@SWNHox (f, g). The 1466-cm^{-1} peak was not observed in those of 3%-C_{60}@SWNHox (e), and 15%- and 40%-C_{60}/as-grown SWNHs (C_{60}/SWNHs) (h and i).

vibration mode of C_{60} when the starting C_{60} concentration was 15 and 40% (Figure 4b,f, g).[22] When the SWNHox was empty (Figure 4a,c) or the C_{60} quantity inside the SWNHox was as small as 3% (Figure 4e), the 1466-cm^{-1} peak ascribed to C_{60} was not seen. The peaks at 1589 and 1346 cm^{-1} were characteristic of SWNH and SWNHox,[12,23,24] and the shoulder

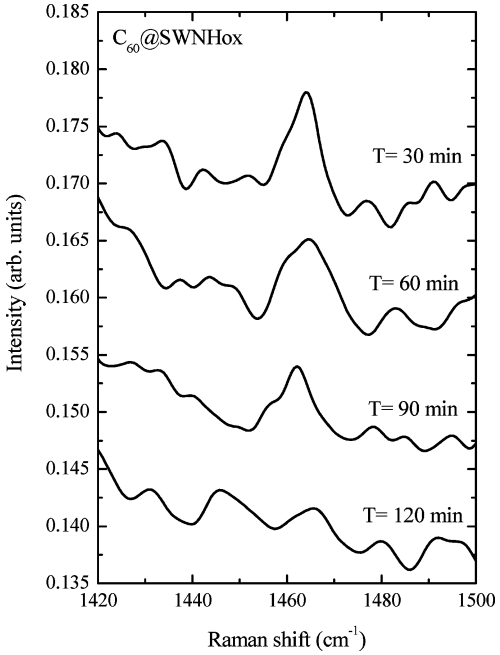

Figure 5. Raman spectra of 15%-C_{60}@SWNHox obtained by repeating measurement continuously. Each measurement took 30 min.

at 1610 cm^{-1} was attributed to the defects in the SWNHox generated by oxygen treatment at 550 °C (Figure 4a−d).[25−27]

An interesting feature of the 1466-cm^{-1} peak ascribed to the C_{60} incorporated inside the SWNHox was that the peak intensity decreased and finally disappeared as the Raman spectrum measurements were continuously repeated, as shown in Figure 5. On the other hand, when C_{60} was located on the outside walls of the as-grown SWNHs, the 1466-cm^{-1} peaks of C_{60} quickly disappeared. In fact, they became very weak or almost invisible as a result of the first scan in the Raman spectrum measurements (Figure 4h,i). Thus, we believe that the 1466-cm^{-1} peak appeared when the C_{60} molecules were incorporated inside the SWNHox in sufficient quantity.

Below, we deduce why the 1466-cm^{-1} peak ascribed to C_{60} disappeared quickly when C_{60} was deposited outside the SWNHox, but slowly when C_{60} was encapsulated inside the SWNHox. It is reported that, when the photopolymerization of the C_{60} molecules occurs by laser irradiation during Raman spectrum measurement, the peak at 1466 cm^{-1} decreases in intensity, increases in width, and shifts to lower frequency, and, in addition, several broader peaks appear near 1466 cm^{-1}.[28−32] Our results agreed with the report that the 1466-cm^{-1} peak of the C_{60} encapsulated inside SWNTs decreases by laser irradiation.[31] In our research, it seems reasonable to believe that the rate of C_{60} photopolymerization outside the SWNHox was faster than that inside the SWNHox, perhaps because the graphene sheets of SWNHox provided optical shielding against laser irradiation for the C_{60} molecules inside the SWNHox.

XRD and Raman-spectrum measurements (Figures 3−5) showed that most of the C_{60} molecules were incorporated inside the SWNHox when the starting quantity of C_{60} was 40% or less.

Controlling the Rate of Release of C_{60}. 15%-C_{60}@SWNHox (0.11-g/g C_{60}@SWNHox, Table 1) was immersed in toluene, and the UV/vis absorption spectra were measured. The C_{60} molecules released in toluene showed an absorption peak at 336 nm, which corresponds to intraband electronic transition of C_{60} (Figure 6a).[33] The absorption intensity increased with the immersion period (Figure 6a). From the maximum-absorbance

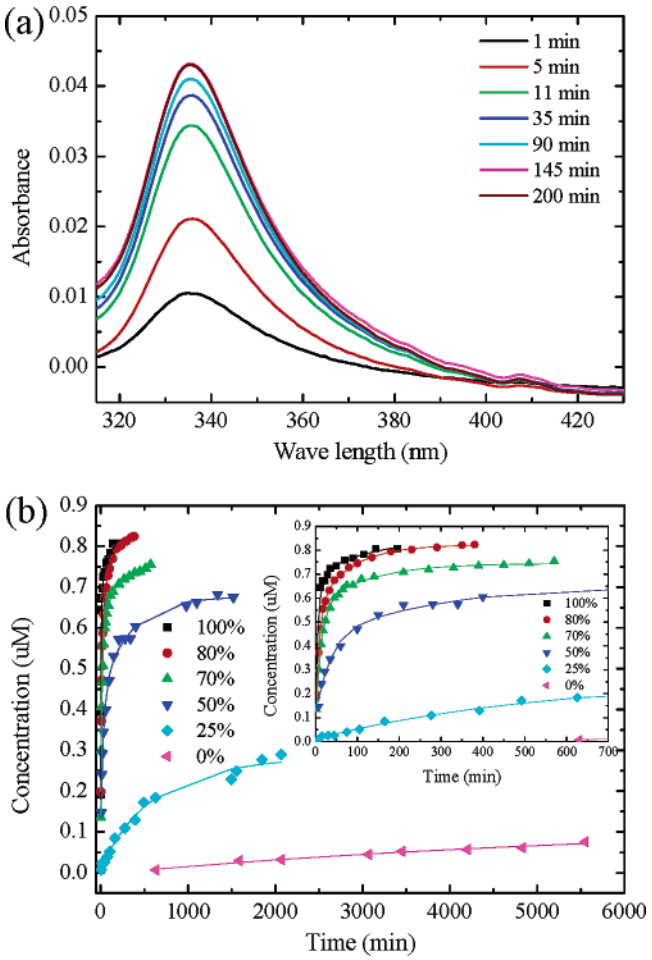

Figure 6. UV/vis absorption spectra of C_{60} released in toluene from 15%-C_{60}@SWNHox by immersion in toluene at various periods (a), and quantities of C_{60} released in toluene, ethanol, and ethanol−toluene solutions, estimated from the maximum absorbance at 336 nm (b). Toluene concentrations of toluene−ethanol solvents were 100% (black), 80% (red), 70% (green), 50% (blue), 25% (pale blue), and 0% (pink). The solid lines in (b) designate the simulation curve for the C_{60}-releasing processes calculated using eq 1.

value at 336 nm in Figure 6a, we estimated the C_{60} concentration dissolved in the toluene. In this estimation, a molar absorption coefficient of C_{60} at 336 nm in toluene, 54000 L mol^{-1} cm^{-1}, was used, which was obtained by our own measurements.[34] This value coincided with the reported value measured for the C_{60} in hexane, 52800 L mol^{-1} cm^{-1}.[33] The concentration of C_{60} dissolved in toluene reached the maximum (about 0.8 μM) in 2 h (Figure 6b, black square). This 0.8 μM concentration corresponded to about 0.11 g/g (underlined in Table 1) for the C_{60}@SWNHox, indicating that most of the C_{60} molecules were released from the SWNHox. An almost empty SWNHox was obtained after the 30-min immersion in toluene, as was confirmed by the TEM observation (Figure 7), the TGA (Figure 2c: C_{60}@SWNHox-tol), and the Raman spectrum (Figure 4d).

Figure 6b shows the immersion-period dependence of the quantity of C_{60} released in toluene, ethanol, and ethanol−toluene solutions. In each solution, the C_{60} released quickly at the beginning, followed by the slow release. As the toluene/ ethanol ratio decreased, the release rate decreased, which would be due to the fact that solubility of the C_{60} decreased at the higher concentrations of ethanol in toluene.[35] The release of the C_{60} from the C_{60}/as-grown-SWNH in toluene was much more rapid and finished in 3 min (not shown). This rapid release is

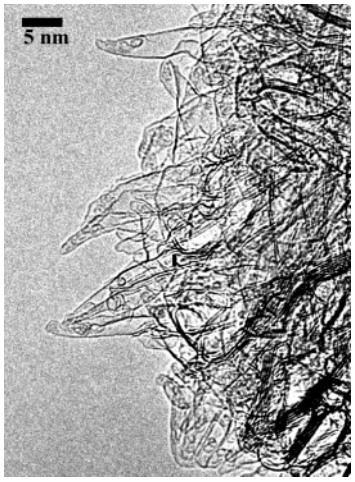

Figure 7. TEM image of 15%-C_{60}@SWNHox after immersion in toluene for 30 min, indicating most C_{60} molecules were released.

discriminated from the slow release of the C_{60} from the inside space of the SWNHox.

The processes involved in the release of C_{60} from C_{60}@SWNHox were analyzed numerically. Since the release profiles for 100−25% concentrations of toluene in Figure 6b consist of the slow and fast components, we assume that each profile is the superposition of the two independent release processes, that is, the releases from the energetically shallow and deep adsorption sites inside the SWNHox, which are expressed as follows:

$$\frac{dn_i}{dt} = -\alpha_i n_i \ (i = 1, 2)$$

$$n_i = P_i e^{-\alpha_i t}$$

$$C = C_0 - P_1 e^{-\alpha_1 t} - P_2 e^{-\alpha_2 t} \qquad (1)$$

Here, "1" and "2" denote the shallow and deep sites inside the SWNHox, respectively. The"n_i" is the quantity of C_{60} at each site inside the SWNHox at time t, and was reduced in units of mol L^{-1} (solvent = 300 cm^3) in the calculation using eq 1. "α_i" and "P_i" indicate the release rate of the C_{60} from the inner space of the SWNHox and the maximum releasable quantities of C_{60} from each site, respectively. The concentration of C_{60} in the solvent was designated as "C" whose initial value was zero, that is, "$C_0 = P_1 + P_2$". The solid lines of Figure 6b show the results of the curve-fitting using the eq 1 with the five adjustable parameters, C_0, α_i and P_i. Since the calculated curves coincided with the experimental points, the assumption that the release proceeded via independent slow and fast processes might be adequate. The value ($P_1 + P_2$) is not much different from C_0 for each concentration of solution, also indicating that the curve-fitting might be adequate.

The value of α_1 was larger than that of α_2 (Table 2), which indicates that the C_{60} was released more quickly from the shallow sites than from the deep sites. The decrease of values of α_1 and α_2 with the decrease of toluene concentration might be reasonable, because the C_{60} solubility in the toluene−ethanol solution decreases.[35]

The values of ($P_1 + P_2$) (or C_0) were close to the initial C_{60} quantities of C_{60}@SWNHox used in the release experiments, that is, 0.8 μM, when the toluene concentration in the toluene/ ethanol solutions were 100, 80, and 70%. This means that most of the C_{60} was released from C_{60}@SWNHox in these three

TABLE 2: Release Rates of C_{60} from the Two Sites inside the SWNHox (α_1 and α_2) and the Releasable-Quantities of C_{60} Released from the Two Sites (P_1 and P_2) Obtained as a Result of Fitting the C_{60}-Release Profiles Shown in Figure 6b to Eq 1

toluene (%) in toluene/ethanol solutions[a]	100%	80%	70%	50%	25%	0%[b]
α_1 (1/min)	0.14	0.10	0.08	0.03	0.002	0.00015
α_2 (1/min)	0.007	0.012	0.009	0.003	0.001	
P_1 (μM)	0.51	0.46	0.49	0.34	0.14	0.13
P_2 (μM)	0.16	0.26	0.19	0.24	0.14	
C_0 (μM)	0.85	0.82	0.74	0.68	0.29	0.13

[a] The suffixes "1" and "2" denote the energetically shallow and deep adsorption sites, respectively. [b] In the case of 0%, the single exponential equation was used for the profile fitting.

toluene−ethanol solutions. The ratio of P_1 to P_2 in the cases of these three solutions were about 2.5:1. We compare this ratio with the previous reports. The theoretical calculation of Okada et al.[36] indicated that the C_{60} encapsulated inside SWNTs is most stable when the SWNT diameter is about 1.4 nm; it becomes unstable as the SWNT diameter increases. On the other hand, the C_{60} distribution inside SWNHox was experimentally studied through the TEM observations by Ajima et al.,[15] in which the C_{60} distribution was shown to depend on the local diameters of SWNHox. Using their results, we estimated the number ratio of C_{60} molecules locating at the local diameters above and below 1.5 nm and found that it was about 1.5:1. This value and our value of 2.5:1 were similar, suggesting that the shallow and deep sites would correspond to the sites with local diameters larger and smaller than 1.4−1.5 nm, respectively.

On the other hand, the values of ($P_1 + P_2$) (or C_0) decreased when the toluene concentration decreased to 50 and 25% because of the lowering of C_{60} solubility. Along with the decrease of the values of $P_1 + P_2$, the ratio P_1:P_2 decreased in the case of the toluene−ethanol solutions with the concentrations of 50 and 25%. This is probably because we ignored several factors in constructing the eq 1, such as, the migration of C_{60} molecules between the two sites inside SWNHox, the interactions of the C_{60} with the solvent molecules inside the SWNHox, and the interaction of the solvent molecules with the inner walls of the SWNHox. To clarify these, further experiments and calculations are necessary.

In the case of 0% toluene, the release profile appears to reflect a single release process. The release profiles were well simulated by the single exponential formula (eq 1). This would mean that the release occurred only from the shallow site "1" in ethanol, which is reasonable for the small affinity of C_{60} with ethanol.[35]

Mechanism of Incorporation and Release. For the nano-precipitation process, we first mixed C_{60}, SWNHox, and toluene and waited until the toluene had completely evaporated. When the toluene had evaporated and the C_{60} concentration reached the solubility limit, the C_{60} began to precipitate at the energetically stable sites, that is, inside the SWNHox. Since the dissolved-concentration limit results in guest molecules becoming incorporated inside the SWNHox, this method is generally applicable to various combinations of molecules and solvents.

The loose contact between the C_{60} and the walls of the SWNHox due to their small curvature enabled oxygen and toluene to permeate the hollow inner spaces of the SWNHox, even when the C_{60} molecules were already incorporated. This would allow the C_{60} molecules to combust independently from the SWNHs during TG measurements (Figure 2) and to be released in toluene and other solvents (Figure 6). The fact that the release rate decreases with the addition of ethanol to toluene (Figure 6b) also suggests that the solution permeates into the C_{60}@SWNHox. The release processes were well reproduced by the two independent processes for the release of C_{60} from the C_{60}@SWNHox into toluene, ethanol, and ethanol−toluene solutions. The calculation indicated various characteristics of the release processes, which we believe were substantially reasonable. However, to enable a more detailed discussion, we need to improve the calculation and method of measuring the quantity of C_{60} that is released.

The importance of the small curvature and large hollow inner spaces of the SWNHs as the recoverable material storage tank are highlighted by the fact that the C_{60} combusts together with the SWNTs[37] and is not released as a result of being immersed in toluene,[38] when the C_{60} molecules were incorporated inside SWNTs that have smaller diameters less than 2 nm, typically, about 1.3 nm.

Conclusion

We used a "nano-precipitation" method to incorporate the C_{60} in the SWNHox and could obtain a large quantity of C_{60}@SWNHox. With this method, the quantity incorporated can be controlled simply by adjusting the starting quantity of C_{60} against the SWNHox. Since "nano-precipitation" is carried out at room temperature in a liquid phase, it is one of the most preferred methods for incorporating organic materials in nanotubes, because many organic materials are thermally unstable and often dissolve in certain solvents. Since the dissolved-concentration limit results in the guest molecules being incorporated inside the SWNHox during the "nano-precipitation" process, this method is generally applicable to various combinations of molecules and solvents.

Control of the release rate of the C_{60} in solutions is possible using solvents with different solubility for C_{60}. C_{60} was released quickly in toluene, but its rate of release became slower with the addition of ethanol to the toluene. The release profiles were reasonably simulated by assuming two independent release processes from the energetically shallow and deep adsorption sites.

The success of controlling the incorporation of C_{60} in SWNHox and its release rate are likely to depend on the small curvature of the inside walls of the SWNHs which holds guest molecules loosely, and their large hollow inner spaces that allow molecules to move with relative freedom.

Acknowledgment. This work was, in part, performed under the management of the Nano Carbon Technology project supported by NEDO. We also thank T. Azami and D. Kasuya for preparing the SWNH samples.

Supporting Information Available: TEM image of residue obtained by stopping TG measurement of C_{60}@SWNHox in helium at 500 °C. This material is available free of charge via the Internet at http:// pubs.acs.org.

References and Notes

(1) Ajayan, P. M.; Iijima, S. *Nature* **1993**, *361*, 333.
(2) Ajayan, P. M.; Ebbesen, T. W.; Ichihashi, T.; Iijima, S.; Tanigaki, K.; Hiura, H. *Nature* **1993**, *362*, 522.
(3) Tsang, S. C.; Chen, Y. K.; Harris, P. J. F.; Green, M. L. H. *Nature* **1994**, *372*, 159.
(4) Hirahara, K.; Suenaga, K.; Bandow, S.; Kato, H.; Okazaki, T.; Shinohara, H.; Iijima, S. *Phys. Rev. Lett.* **2000**, *85*, 5384.
(5) Smith, B. W.; Monthioux, M.; Luzzi, D. E. *Nature* **1998**, *396*, 323.
(6) Meyer, R. R.; Sloan, J.; Dunin-Borkowski, R. E.; Kirkand, A. I.; Novotny, M. C.; Bailey, S. R.; Hutchison, J. L.; Green, M. L. H. *Science* **2000**, *289*, 1324.

(7) Gao, Y.; Bando, Y. *Nature* **2002**, *415*, 599.
(8) Takenobu, T.; Takano, T.; Shiraishi, M.; Murakami, Y.; Ata, M.; Kataura, H.; Achiba, Y.; Iwasa, Y. *Nat. Mater.* **2003**, *2*, 683.
(9) Yudasaka, M.; Ajima, K.; Suenaga, K.; Ichihashi, T.; Hashimoto, A.; Iijima, S. *Chem. Phys. Lett.* **2003**, *380*, 42.
(10) Simon, F.; Kuzmany, H.; Rauf, H.; Pichler, T.; Bernardi, J.; Peterlik, H.; Korecz, L.; Fülöp, F.; Janossy, A. *Chem. Phys. Lett.* **2004**, *383*, 362.
(11) Thamavaranukup, N.; Höppe, H. A.; Ruiz-Gonzalez, L.; Costa, P. M. F. J.; Sloan, J.; Kirkland, A.; Green, M. L. H. *Chem. Commun.* **2004**, 1686.
(12) Iijima, S.; Yudasaka, M.; Yamada, R.; Bandow, S.; Suenaga, K.; Kokai, F.; Takahashi, K. *Chem. Phys. Lett.* **1999**, *309*, 165.
(13) Murata, K.; Kaneko, K.; Steele, W. A.; Kokai, F.; Takahashi, K.; Kasuya, D.; Hirahara, K.; Yudasaka, M.; Iijima, S. *J. Phys. Chem. B* **2001**, *105*, 10210.
(14) Bekyarova, E.; Murata, K.; Yudasaka, M.; Kasuya, D.; Iijima, S.; Tanaka, H.; Kahoh, H.; Kaneko, K. *J. Phys. Chem. B* **2003**, *107*, 4681.
(15) Ajima, K.; Yudasaka, M.; Suenaga, K.; Kasuya, D.; Azami, T.; Iijima, S. *Adv. Mater.* **2004**, *16*, 397.
(16) Hashimoto, A.; Yorimitsu, H.; Ajima, K.; Suenaga, K.; Isobe, H.; Miyawaki, J.; Yudasaka, M.; Iijima, S.; Nakamura, E. *Proc. Natl. Acad. Sci.* **2004**, *101*, 8527.
(17) Yuge, R.; Ichihashi, T.; Shimakawa, Y.; Kubo, Y.; Yudasaka, M.; Iijima, S. *Adv. Mater.* **2004**, *16*, 1420.
(18) Murata, K.; Hashimoto, A.; Yudasaka, M.; Kasuya, D.; Kaneko, K.; Iijima, S. *Adv. Mater.* **2004**, *16*, 1520.
(19) Murakami, T.; Ajima, K.; Miyawaki, J.; Yudasaka, M.; Iijima, S.; Shiba, K. *Mol. Pharm.* **2004**, *1*, 399.
(20) Fan, J.; Yudasaka, M.; Kasuya, D.; Azami, T.; Yuge, R.; Imai, H.; Kubo, Y.; Iijima, S. *J. Phys. Chem. B* **2005**, *109*, 10756.
(21) Klein, C. A. *Electrical Properties of Pyrolytic Graphite in Organic Semiconductors*; Brophy, J. J., Buttrey, J. W., Eds.; Macmillan: New York, 1964.
(22) Eklund, P. C.; Zhou, P.; Wang, K.-A.; Dresselhaus, G.; Dresselhaus, M. S. *J. Phys. Chem. Solids* **1992**, *53*, 1391.
(23) Tuinstra, F.; Koenig, J. L. *J. Chem. Phys.* **1970**, *53*, 1126.
(24) The peak at 1589 cm^{-1} corresponds to the in-plane stretching (E_{2g} symmetry) mode of graphite, and that at 1346 cm^{-1} is attributed to the Raman inactive A_{1g} mode that becomes Raman active by symmetry breaks at the edges of small graphite crystallites (ref 23).
(25) Kasuya, D.; Yudasaka, M.; Takahashi, K.; Kokai, F.; Iijima, S. *J. Phys. Chem. B* **2002**, *106*, 4947.
(26) Nakamizo, M.; Honda, H.; Inagaki, M. *Carbon* **1978**, *16*, 281.
(27) Nakamizo, M.; Tamai, K. *Carbon* **1984**, *22*, 197.
(28) Rao, A. M.; Zhou, P.; Wang, K.-A.; Hager, G. T.; Holden, J. M.; Wang, Y.; Lee, W. T.; Bi, X.-X.; Eklund, P. C.; Cornett, D. S.; Duncan, M. A.; Amster, I. J. *Science* **1993**, *259*, 955.
(29) Matsuishi, K.; Ohno, T.; Yasuda, N.; Nakanishi, T.; Onari, S.; Arai, T. *J. Phys. Chem. Solids* **1997**, *58*, 1747.
(30) Zhou, P.; Rao, A. M.; Wang, K.-A.; Robertson, J. D.; Eloi, C.; Meier, M. S.; Ren, S. L., Bi, X.-X.; Eklund, P. C.; Dresselhaus, M. S. *Appl. Phys. Lett.* **1992**, *60*, 2871.
(31) Kataura, H.; Maniwa, Y.; Abe, M.; Fujiwara, A.; Kodama, T.; Kikuchi, K.; Imahori, H.; Misaki, Y.; Suzuki, S.; Achiba, Y. *Appl. Phys. A* **2002**, *74*, 349.
(32) Matus, M.; Kuzmany, H. *Appl. Phys. A* **1993**, *56*, 241.
(33) Bensasson, R. V.; Hill, T. J.; Land, E. J.; Leach, S.; McGarvey, D. J.; Truscott, T. G.; Ebenhoch, J.; Gerst, M.; Rüchardt, C. *Chem. Phys.* **1997**, *215*, 111.
(34) The molar absorption coefficient was estimated through the measurements of the UV/vis absorption spectra of C_{60} dissolved in toluene with various concentrations by applying the Lambert−Beer relation to the maximum absorbance values at the 336-nm peak, which is ascribed to the electronic transition of C_{60}.
(35) Ruoff, R. S.; Tse, D. S.; Malhotra, R.; Lorents, D. C. *J. Phys. Chem.* **1993**, *97*, 3379.
(36) Okada, S.; Otani, M.; Oshiyama, A. *Phys. Rev. B.* **2003**, *67*, 205411.
(37) Zhang, M.; Yudasaka, M.; Bandow, S.; Iijima, S. *Chem. Phys. Lett.* **2003**, *369*, 680.
(38) Kataura, H.; Maniwa, Y.; Kodama, T.; Kikuchi, K.; Hirahara, K.; Suenaga, K.; Iijima, S.; Suzuki, S.; Achiba, Y.; Krätschmer, W. *Synth. Met.* **2001**, *121*, 1195.